Optik 82, No. 3 (1989) 99–113

Second order transfer matrices for inhomogeneous field Wien filters including spin-precession

M. R. Scheinfein

National Institute of Standards and Technology (formerly National Bureau of Standards) Gaithersburg, MD USA

Received February 20, 1989

Abstract

Second order transfer matrices for inhomogeneous field Wien filters including spin-precession. Inhomogeneous field Wien filters offer an alternative to the conventional uniform field Wien filter, magnetic sector or electrostatic deflector for electron-spin rotation. Their main advantage is the point-to-point stigmatic focusing property which preserves the cylindrical symmetry in a beam transport system. Both uniform and inhomogeneous field Wien filters may be used for spin rotation and/or energy/mass analysis. The complete transfer matrix of a general inhomogeneous field Wien filter is derived in a second order approximation. The matrix elements for the precession of the electron spin-polarization vector are included in a separate spin-rotation matrix. Real entrance and exit fringing fields are included for the specialized case of a Wien filter with curved and normal (not inclined) entrance and exit pole faces. The transfer matrices are parameterized in terms of beam parameters and the multipole expansion coefficients of the filter's electric and magnetic fields.

Inhalt

Transfermatrizen 2. Ordnung von Wien-Filtern für inhomogene Felder und Spin-Präzession. Wien-Filter für inhomogene Felder sind eine Alternative zu den konventionellen Wien-Filtern für homogene Felder, magnetischer Sektor oder elektrostatische Ablenksysteme für Elektronenspin-Rotation. Ihr wichtigster Vorteil ist die stigmatische Punkt-zu-Punkt Fokusiereigenschaft, die die Zylindersymmetrie im Strahltransportsystem bewahrt. Wien-Filter für uniforme wie für inhomogene Felder können zur Analyse der Spin-Rotation und/oder der Energie/Masse verwendet werden. Die vollständige Transfermatrize eines Wien-Filters für inhomogene Felder wird in einer Näherung zweiter Ordnung abgeleitet. Die Matrizenelemente für die Präzession des Elektronen-Spin-Polarisationsvektors sind in einer separaten Spin-Rotations-Matrize enthalten. Reelle Eingangs- und Ausgangsfelder sind für den speziellen Fall eines Wien-Filters mit gekrümmten und normalen (nicht gekippten) Eingangs- und Ausgangspolebenen mitberücksichtigt. Die Transfermatrizen sind parametrisiert in Termen der Strahlparameter und der Koeffizienten der Multipolerweiterung der elektrischen und magnetischen Felder des Filters.

1. Introduction

The velocity filter formed from crossed electric and magnetic fields has become known as the Wien filter [1]. The Wien filter has been used as an electron energy loss spectrometer and monochromator [2, 3, 4, 5, 6], mass filter and ion separator [7, 8, 9, 10], and an electron-spin rotator [11, 12, 13]. The original theory was developed largely for the homogeneous field Wien filter [14, 15, 16, 17, 18, 19, 20] which suffers from the limitation that it focuses only in one direction, thus forming a line image at the image plane. The main advantage of inhomogeneous field Wien filters used as both analyzers and spin rotators are their ability to perform point-to-point focusing [21, 22, 23, 24, 25, 26, 27].

In addition to the double focusing property of inhomogeneous field Wien filters, these devices have another salient feature which we would like to exploit. Wien filters utilize an electric field whose strength is adjusted to keep the charged particle trajectories in a straight line while passing through the magnetic field. Thus, the central axis trajectory throug the Wien filter is a straight line. It will be shown that the zeroeth order trajectory displacement and first order tilt due to the entrance and exit fringe fields can be eliminated. This is attractive from the standpoint of alignment and interfacing the Wien filter with auxilliary optics.

The Wien filter can be operated in several modes. If the incident energy of the beam is large, the Wien filter may be operated as an electron-spin rotator or an electron spectrometer/mass filter with small dispersion. When the Wien filter is operated with low incident energies, utilizing a pre-retardation lens [4, 6, 27], much higher dispersion can be achieved. High resolution electron energy loss spectroscopy or high resolution mass analysis usually exploits the high performance of the Wien filter with pre-retardation. For all applications, it is desirable to have high transmission through the device. It is this requirement which constrains us to consider higher order aberrations.

In this report, the complete second order transfer matrices for inhomogeneous field Wien filters are derived, including the matrix which governs the precession of the electron-spin. The effects of the fringing fields at the entrance and exit of the filter are included. The transfer matrices for the spatial trajectories are derived using the trajectory method and expanding the electric and magnetic fields into multipole components. The real fields can be formed by suitably placed (multipole) coils and electrodes [26, 27], cylindrical condensers and tilted/curved magnetic pole pieces [5, 22, 23, 27] or in toroidal fields using imbedded electrodes [24, 25]. Once the second order trajectories through the Wien filter are known, the coupled differential equations governing the electron-spin precession in inhomogeneous fields can be solved using the trajectory method.

M. R. Scheinfein, National Institute of Standards and Technology (formerly National Bureau of Standards) Gaithersburg, MD 20899, USA

2. Multipole field expansions

We begin the analysis of the trajectories in an inhomogeneous field Wien filter by expressing the potentials and fields in terms of multipole expansions. The geometry used for the derivation of the Wien filter transfer matrices has the dominant dipole fields oriented in the $x-y$ plane. The primary electron ray trajectory is directed in the positive z-direction and lies on the z-axis, passing through (0, 0) in the $x-y$ plane. In fig. 1, two of several possible variations are given for realizing the fields in an inhomogeneous field Wien filter. In one case, fig. 1a, the inhomogeneous fields are excited by curved electrodes and tilted magnetic pole pieces, whereas in a second option, fig. 1b, the fields are excited by suitably superimposed excitations (U_i and I_i are the potentials and amp-turn flux linkages for each individual pole. Specific excitations [29, 30] are required to excite the particular multipole fields which may be superimposed on one another.) of the electric/magnetic octupole. The dipole fields in fig. 1a and 1b are oriented such that in the midplane

$$\boldsymbol{E}_{\text{dipole}} = \hat{x} E_1 \qquad \boldsymbol{B}_{\text{dipole}} = \hat{y} B_1. \tag{1}$$

The subscript "1" refers to the dipole component of the field and the coefficients E_1 and B_1 are real and positive parameters that depend only on z. Throughout this paper we will refer to the charged particle as an electron. Although the extension to general charged particles is implied, the negative electronic charge of the electron has been incorporated into the equations. With this dipole field orientation, the electrical force on an electron is in the negative x-direction while the magnetic force is in the positive x-direction. The x-direction is the dispersion direction. The balancing condition, or the zeroeth order Wien filter focusing condition, where the magnetic and electrical forces are equal occurs when

$$evB_1 = eE_1 \quad \text{or} \quad \sqrt{2\eta\phi_o}\,B_1 = E_1. \tag{2}$$

$\eta = -e/m$ is the charge to mass ratio and ϕ_o is the initial electron (electric) potential set such that the initial kinetic energy K_o is given by $e\phi_o$.

We wish to express the components of the fields in terms of two dimensional multipole field expansions greatly simplifying the ensuing analysis. The fields are defined as the negative gradient of the electric and magnetic scalar potentials ϕ and ψ for each multipole component [28]. The polar angle α is measured from the positive x-axis in the usual way. Superscripts in parentheses denote differentiation with respect to z

$$\boldsymbol{E} = -\nabla\phi = -\nabla \sum_{n=0}^{\infty} \phi_n = -\nabla \sum_{n=0}^{\infty} \sum_{p=0}^{\infty} \frac{(-1)^p (-E_n)^{(2p)} r^{2p+n} \cos(n\alpha)}{4^p\, p!(n+1)(n+2)\dots(n+p)}, \tag{3}$$

$$\boldsymbol{B} = -\mu_o\nabla\psi = -\mu_o\nabla \sum_{n=0}^{\infty} \psi_n = -\mu_o\nabla \sum_{n=0}^{\infty} \sum_{p=0}^{\infty} \frac{(-1)^p (-B_n)^{(2p)} r^{2p+n} \sin(n\alpha)}{\mu_o 4^p\, p!(n+1)(n+2)\dots(n+p)}. \tag{4}$$

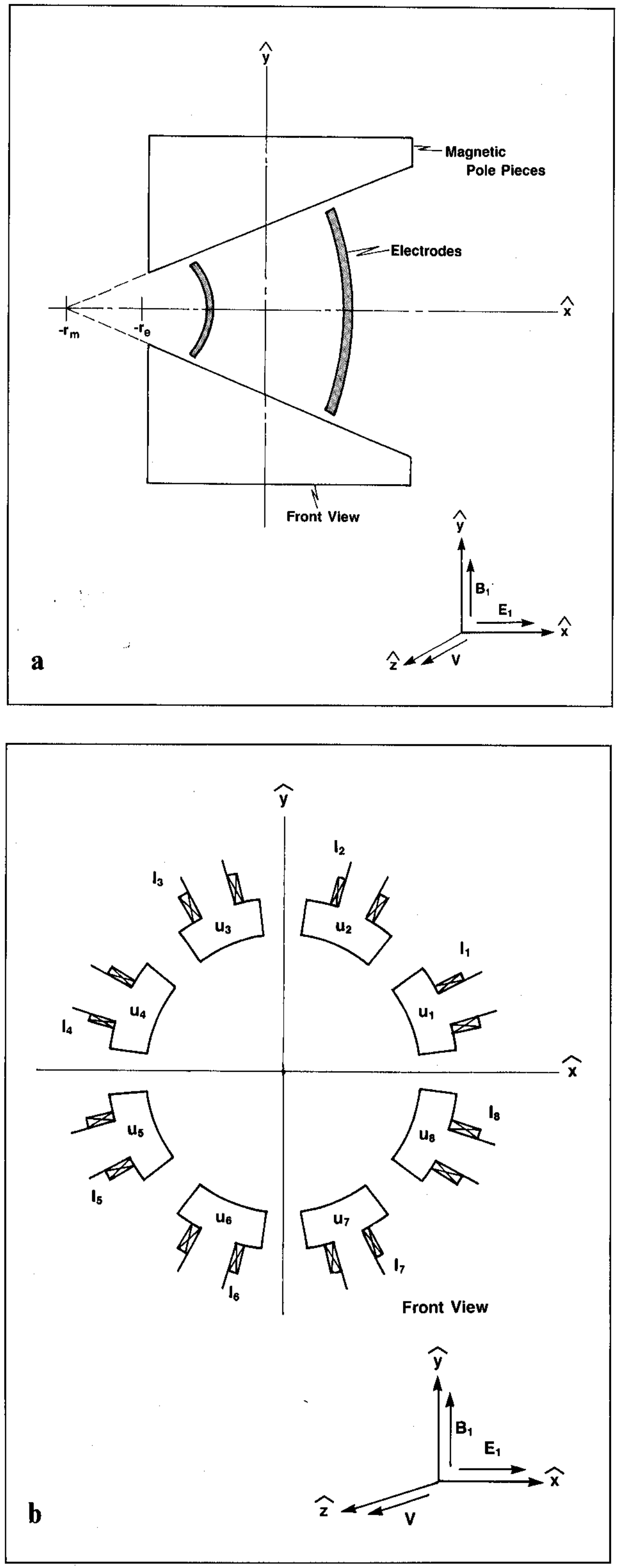

Fig. 1. (a) Tilted magnetic poles and curved electrodes used for the realization of the multipole fields in an inhomogeneous field Wien filter. The dipole fields are oriented in the $x-y$ plane and the electron trajectory is in the positive z direction. (b) An octupole system for realizing the Wien filter fields.

Primes will be used exclusively to denote differentiation with respect to z where z is the distance along the optic axis (central or primary ray) as defined in fig. 1. Explicit expressions for the electric and magnetic multipole potential expansions are given below in a third order approximation [26]. The numerical subscript defines the multipole field order.

Dipole Components:

$$\phi_1 = \phi_o - \left[E_1 - \frac{1}{8}E_1''(x^2+y^2)\right]x + \cdots, \tag{5}$$

$$\psi_1 = -\frac{1}{\mu_o}\left[B_1 - \frac{1}{8}B_1''(x^2+y^2)\right]y + \cdots. \tag{6}$$

Quadrupole Components:

$$\phi_2 = -\left[E_2 - \frac{1}{12}E_2''(x^2+y^2)\right](x^2-y^2) + \cdots, \tag{7}$$

$$\psi_2 = -\frac{2}{\mu_o}\left[B_2 - \frac{1}{12}B_2''(x^2+y^2)\right]xy + \cdots. \tag{8}$$

Hexapole Components:

$$\phi_3 = -E_3(x^3 - 3xy^2) + \cdots, \tag{9}$$

$$\psi_3 = -\frac{1}{\mu_o}B_3(3x^2y - y^3) + \cdots. \tag{10}$$

We want to express the potentials and the fields as a function of the multipole expansion coefficients in complex notation such that the transverse coordinates x and y can be included in a single differential equation. To do this, we define the following standard coordinate transformation: $\omega = x + iy$, $\bar{\omega} = x - iy$ and $z = z$. The fields can also be expressed in complex form. In our convention, $E_\omega = E_x + iE_y$ and $B_\omega = B_x + iB_y$ and the fields are derived from the scalar potentials as

$$E_\omega = -2\frac{\partial\phi}{\partial\bar{\omega}}, \quad E_z = -\frac{\partial\phi}{\partial z},$$
$$B_\omega = -2\mu_o\frac{\partial\psi}{\partial\bar{\omega}}, \quad B_z = -\mu_o\frac{\partial\psi}{\partial z}. \tag{11}$$

When the potentials and fields are expressed in terms of the complex transverse coordinates ω and $\bar{\omega}$ and the multipole field coefficients, and terms of third order in the potentials and second order in the fields are retained, the following general expressions for the excitation of the Wien filter potentials and fields results

$$\phi = \phi_o - \tfrac{1}{2}[E_1(\omega+\bar{\omega}) + E_2(\omega^2+\bar{\omega}^2) + E_3(\omega^3+\bar{\omega}^3) - \tfrac{1}{8}E_1''(\omega^2\bar{\omega} + \omega\bar{\omega}^2)], \tag{12}$$

$$\psi = \frac{i}{2\mu_o}[B_1(\omega-\bar{\omega}) + B_2(\omega^2-\bar{\omega}^2) + B_3(\omega^3-\bar{\omega}^3) - \tfrac{1}{8}B_1''(\omega^2\bar{\omega} - \omega\bar{\omega}^2)], \tag{13}$$

$$E_\omega = E_1 + 2E_2\bar{\omega} + 3E_3\bar{\omega}^2 - \tfrac{1}{8}E_1''(\omega^2 + 2\omega\bar{\omega}), \tag{14}$$

$$E_z = \tfrac{1}{2}[E_1'(\omega+\bar{\omega}) + E_2'(\omega^2+\bar{\omega}^2)], \tag{15}$$

$$B_\omega = i[B_1 + 2B_2\bar{\omega} + 3B_3\bar{\omega}^2 + \tfrac{1}{8}B_1''(\omega^2 - 2\omega\bar{\omega})], \tag{16}$$

$$B_z = -\frac{i}{2}[B_1'(\omega-\bar{\omega}) + B_2'(\omega^2-\bar{\omega}^2)]. \tag{17}$$

3. Second order trajectory equation

The complex all orders trajectory equation for transverse motion of an electron with coordinates $(\omega, \bar{\omega})$, parameterized in z, is derived from the Lorentz force equation [26]

$$\frac{d}{dz}\left[\frac{\sqrt{\phi}\,\omega'}{\sqrt{1+\omega'\bar{\omega}'}}\right] = -\frac{E_\omega}{2\sqrt{\phi}}\sqrt{1+\omega\bar{\omega}} + i\sqrt{\frac{\eta}{2}}[\omega' B_z - B_\omega]. \tag{18}$$

To develop a second order theory, we must expand all terms in the differential equation containing ω and $\bar{\omega}$ to second order.

As before (eq. 2) we set $\phi_o = K_o/e$ and incorporate the initial energy spread of the beam with $\phi_o \Rightarrow \phi_o(1+\delta)$ where δ is $\Delta K/K_o$. This term will give rise to dispersion, a characteristic parameter for energy loss spectrometers. The expansions for the potential, electric and magnetic fields given in equations (12–17) must be inserted into the trajectory equation (18) to form the complete second order inhomogeneous Wien filter trajectory equation. This second order expanded differential equation is the starting point for the present analysis and is given below. (Note: This is a more precise version of the Wien filter equation originally given as equation (9) in reference 26; the earlier equation is missing second order terms and does not handle terms due to energy variation rigorously)

$$\omega'' + \frac{\bar{\omega}}{\phi_o}\left[E_2 - \sqrt{2\eta\phi_o}\,B_2 + \frac{E_1^2}{8\phi_o}\right] + \frac{E_1^2\omega}{8\phi_o^2} = \frac{E_1\delta}{4\phi_o} + F_2(\omega, z),$$

$$\begin{aligned} F_2(\omega,z) = -\frac{1}{4\phi_o} \cdot \Bigg\{ & \omega'^2[-E_1] + \omega^2\left[\frac{E_1E_2}{2\phi_o} + \frac{5E_1^3}{16\phi_o^2} - \sqrt{\frac{\eta\phi_o}{2}}\,B_1''\right] \\ & + \bar{\omega}^2\left[\frac{5E_1E_2}{2\phi_o} + \frac{5E_1^3}{16\phi_o^2} + 6E_3 - 6\sqrt{2\eta\phi_o}\,B_3 - \frac{E_1}{\phi_o}\sqrt{2\eta\phi_o}\,B_2\right] \\ & + \omega\bar{\omega}\left[\frac{5E_1^3}{8\phi_o^2} + \frac{2E_1E_2}{\phi_o} - \frac{E_1}{\phi_o}\sqrt{2\eta\phi_o}\,B_2\right] \\ & + \omega'\omega[-2E_1'] + \omega\delta\left[-\frac{5E_1^2}{4\phi_o}\right] \\ & + \bar{\omega}\delta\left[2\sqrt{2\eta\phi_o}\,B_2 - 4E_2 - \frac{5E_1^2}{4\phi_o}\right] + \delta^2\left[\frac{5E_1}{4}\right]\Bigg\}. \end{aligned} \tag{19}$$

4. Solutions to the trajectory equation

In order to form a stigmatic focusing system, the first order trajectory equation (equation (19) with $F_2 = 0$ and $\delta = 0$) must be identical for both x and y coordinates. This condition is the first order Wien filter focusing condition. Mathematically, this criterion is satisfied when the following equation is met

$$E_2 - \sqrt{2\eta\,\phi_o}\,B_2 + \frac{E_1^2}{8\phi_o} = 0. \tag{20}$$

For the stigmatic focusing system, ignoring aberrations ($F_2 = 0$), the equation governing the motion of the electrons in the fields is simply

$$\omega'' + \frac{E_1^2}{8\phi_o^2}\,\omega = \frac{E_1\delta}{4\phi_o} \quad \text{or} \quad \omega'' + \frac{\eta B_1^2}{4\phi_o} = \frac{E_1\delta}{4\phi_o} \tag{21}$$

where the balancing condition has been used. We will choose solutions to this simplified equation (21) of the following form

$$\omega = \omega_o\,g(z) + \omega_o'\,h(z) + \delta d(z). \tag{22}$$

The subscripted variables represent the initial conditions. The two functions, $g(z)$ and $h(z)$, are real. The $d(z)$ term, also real, represents the dispersion and results from the first order term on the right hand side of equation (21). Traditionally, the solutions $g(z)$ and $h(z)$ are given for the following initial conditions, where z_o defines the starting position (outside of the Wien filter fields) along the optic axis

$$g(z_o) = h'(z_o) = 1, \quad g'(z_o) = h(z_o) = d(z_o) = d'(z_o) = 0. \tag{23}$$

We can rewrite the paraxial equation of motion for an electron of fixed energy ($\delta = 0$) as $\omega'' + k^2\omega = 0$ where $k^2 = \eta B_1^2/4\phi_o = E_1^2/8\phi_o^2 = 1/2R_o^2$. R_o is the cyclotron radius for the case where the fields are uniform along the length of the Wien filter and constitutes the basic unit of length for the ensuing analysis. Substituting the initial conditions for the general first order trajectory solutions given above, the expressions for the ray-trajectory solutions become (in the *SCOFF* or *S*harp *C*ut *O*ff *F*ringing *F*ield approximation where B and E are independent of z throughout the entire effective length of the Wien filter)

$$g(z) = \cos(kz), \quad h(z) = \frac{1}{k}\sin(kz). \tag{24}$$

The structure of the aberration coefficients and the dispersion term can be generated from a Taylor series expansion. The aberration coefficients, or second order matrix elements must be calculated by taking the integrals of the appropriate forcing functions [31]. The general expansions for the ray equation solutions for a system with dipole symmetry to second order have the following form

$$\begin{aligned} x &= \textstyle\sum (x\,|\,x_o^i y_o^j x_o'^k y_o'^l \delta^m)\,x_o^i y_o^j x_o'^k y_o'^l \delta^m \\ &= (x\,|\,x_o)\,x_o + (x\,|\,x_o')\,x_o' + (x\,|\,\delta)\,\delta + (x\,|\,x_o^2)\,x_o^2 \\ &\quad + (x\,|\,y_o^2)\,y_o^2 + (x\,|\,x_o'^2)\,x_o'^2 + (x\,|\,y_o'^2)\,y_o'^2 \\ &\quad + (x\,|\,x_o x_o')\,x_o x_o' + (x\,|\,y_o y_o')\,y_o y_o' + (x\,|\,x_o\delta)\,x_o\delta \\ &\quad + (x\,|\,x_o'\delta)\,x_o'\delta + (x\,|\,\delta^2)\,\delta^2, \end{aligned} \tag{25}$$

$$\begin{aligned} y &= \textstyle\sum (y\,|\,x_o^i y_o^j x_o'^k y_o'^l \delta^m)\,x_o^i y_o^j x_o'^k y_o'^l \delta^m \\ &= (y\,|\,y_o)\,y_o + (y\,|\,y_o')\,y_o' + (y\,|\,x_o y_o)\,x_o y_o \\ &\quad + (y\,|\,x_o' y_o)\,x_o' y_o + (y\,|\,x_o y_o')\,x_o y_o' \\ &\quad + (y\,|\,x_o' y_o')\,x_o' y_o' + (y\,|\,y_o\delta)\,y_o\delta + (y\,|\,y_o'\delta)\,y_o'\delta. \end{aligned} \tag{26}$$

The terms in parentheses are the matrix elements which relate the initial conditions given by the 'o' subscripted variables to the positions and slopes within the Wien filter or at the exit plane. These matrix elements are what we would like to determine. If $g(z)$ and $h(z)$ are the solutions to the homogeneous differential equation, then each term on the right hand side of equation (19) contributes to the solution of the second order trajectory equation. Assume that each term on the right hand side of equation (19) can be denoted by an arbitrary function of the positions and slopes $F(\omega, \omega', z) = F$. Each of these functions will be termed a forcing function and the matrix element due to that particular forcing function of the second order ray equation (for stigmatic imaging) is given by ω_F, [31] where

$$\omega_F = h(z)\int_0^z F(\omega, \omega', \tau)\,g(\tau)\,d\tau - g(z)\int_0^z F(\omega, \omega', \tau)\,h(\tau)\,d\tau, \tag{27}$$

and where the upper limit of integration is a point z where the electron position is to be evaluated within the Wien filter, or z is the effective length of the Wien filter for evaluation of the electron position at the exit of the filter. Differentiation of this expression twice with respect to z reveals that ω_F satisfies the differential equation for that particular forcing function. When the forcing function F is the term multiplying δ,

$$F \rightarrow \frac{E_1}{4\phi_o} = \frac{1}{2R_o} = \frac{k}{\sqrt{2}} \equiv f \tag{28}$$

we determine the first order dispersion function, $d(z)$,

$$d(z) = \frac{f}{k^2}\,(1 - \cos(kz)). \tag{29}$$

$f = k/\sqrt{2}$ will be used exclusively to designate the dispersion forcing function. It is noted that the mass dispersion term is identical to the energy dispersion term in magnitude, but the sign will be changed.

5. Aberration forcing function coefficients and matrix elements

In order to solve the trajectory equation for the inhomogeneous terms in equation (19), we substitute the first order solutions into the equation and collect terms to determine the forcing functions. The total forcing function is the result of this expansion and is given below in terms of the complex transverse coordinates

$$
\begin{aligned}
F_2(\omega, z) = {} & \omega_o^2[Ag'^2 + Bg^2 + Egg'] + \bar{\omega}_o^2[Cg^2] + \omega_o\bar{\omega}_o[Dg^2] \\
& + \omega_o'^2[Ah'^2 + Bh^2 + Ehh'] + \bar{\omega}_o'^2[Ch^2] \\
& + \omega_o\omega_o'[2Ag'h' + 2Bgh + E(g'h + gh')] \\
& + \omega_o\bar{\omega}_o'[Dgh] + \omega_o'\bar{\omega}_o[Dgh] + \bar{\omega}_o\bar{\omega}_o'[2Cgh] \\
& + \omega_o'\bar{\omega}_o'[Dh^2] + \omega_o\delta[2Ag'd' + 2Bgd + Dgd \\
& \qquad + E(gd' + g'd) + Fg] \\
& + \bar{\omega}_o\delta[2Cgd + Dgd + Gg] \\
& + \bar{\omega}_o'\delta[2Chd + Dhd + Gh] \\
& + \omega_o'\delta[2Ah'd' + 2Bhd + Dhd \\
& \qquad + E(hd' + h'd) + Fh] \\
& + \delta^2[Ad'^2 + Bd^2 + Cd^2 + Dd^2 + Edd' \\
& \qquad + Fd + Gd + H].
\end{aligned}
\tag{30}
$$

The forcing function coefficients are

$$
\begin{aligned}
A &= \frac{E_1}{4\phi_o} \\
B &= -\frac{1}{4\phi_o}\left[\frac{E_1E_2}{2\phi_o} - \sqrt{\frac{\eta\phi}{2}}B_1'' + \frac{5E_1^3}{16\phi_o^2}\right] \\
C &= -\frac{1}{4\phi_o}\left[\frac{5E_1E_2}{2\phi_o} + 6E_3 - 6\sqrt{2\eta\phi_o}B_3 \right. \\
&\qquad \left. - \frac{E_1}{\phi_o}\sqrt{2\eta\phi_o}B_2 + \frac{5E_1^3}{16\phi_o^2}\right] \\
D &= -\frac{1}{4\phi_o}\left[\frac{2E_1E_2}{\phi_o} - \frac{E_1}{\phi_o}\sqrt{2\eta\phi_o}B_2 + \frac{5E_1^3}{8\phi_o^2}\right] \\
E &= \frac{E_1'}{2\phi_o} \\
F &= \frac{5E_1^2}{16\phi_o^2} \\
G &= -\frac{1}{4\phi_o}\left[2\sqrt{2\eta\phi_o}B_2 - \frac{5E_1^2}{4\phi_o} - 4E_2\right] \\
H &= -\frac{5E_1}{16\phi_o}.
\end{aligned}
\tag{31}
$$

Now, we make the substitutions for the complex transverse coordinates and find the forcing functions in terms of the cartesian coordinates.

x-Forcing Functions:

$$
\begin{aligned}
F_2(x_o^2) &= [(B + C + D)g^2 + Egg' + Ag'^2] \\
F_2(y_o^2) &= [(D - B - C)g^2 - Egg' - Ag'^2] \\
F_2(x_o'^2) &= [(B + C + D)h^2 + Ehh' + Ah'^2] \\
F_2(y_o'^2) &= [(D - B - C)h^2 - Ehh' - Ah'^2] \\
F_2(x_ox_o') &= [2(B + C + D)gh + E(gh' + g'h) + 2Ag'h'] \\
F_2(y_oy_o') &= [2(D - B - C)gh - E(gh' + g'h) - 2Ag'h'] \\
F_2(x_o\delta) &= [2(B + C + D)gd + E(gd' + g'd) \\
&\qquad + 2Ag'd' + (F + G)g] \\
F_2(x_o'\delta) &= [2(B + C + D)hd + E(hd' + h'd) \\
&\qquad + 2Ah'd' + (F + G)h] \\
F_2(\delta^2) &= [(B + C + D)d^2 + Edd' + (F + G)d + H].
\end{aligned}
\tag{32}
$$

y-Forcing Functions:

$$
\begin{aligned}
F_2(x_oy_o) &= [2(B - C)g^2 + 2Egg' + 2Ag'^2] \\
F_2(x_o'y_o) &= [2(B - C)h^2 + 2Ehh' + 2Ah'^2] \\
F_2(x_oy_o') &= [2(B - C)gh + E(gh' + g'h) + 2Ag'h'] \\
F_2(x_o'y_o) &= [2(B - C)gh + E(gh' + g'h) + 2Ag'h'] \\
F_2(y_o\delta) &= [2(B - C - D)gd + E(gd' + g'd) \\
&\qquad + 2Ag'd' + (F - G)g] \\
F_2(y_o'\delta) &= [2(B - C - D)hd + E(hd' + h'd) \\
&\qquad + 2Ah'd' + (F - G)h].
\end{aligned}
\tag{33}
$$

These equations are completely general in the sense that the functions $g(z)$, $h(z)$ and $d(z)$ are still arbitrary solutions to the first order equations. If the variable k is dependent on z as $k(z)$, then the solutions will not be given in terms of simple functions as given in equations (24) and (29). However, given any other functional form of the first order solutions, the above forcing functions remain valid. When the fields are uniform in the z direction, which is the case in a Wien filter with a large length to gap ratio, then we can substitute the first order solutions to the trajectory equation given in (24) and (29) into the above expressions. This is the *SCOFF* approximation. In this case we can simplify the expressions for the forcing functions by replacing the expressions for the derivatives of the first order solutions as $g'(z) = -k\sin(kz) \equiv -k^2h$, $h'(z) = \cos(kz) \equiv g$ and $d'(z) = f\sin(kz)/k \equiv fh$. With these substitutions, the final expressions for the complete second order forcing functions for an inhomogeneous field Wien filter in the *SCOFF* approximation are given in (34) and (35) below.

x-Forcing Functions:

$$
\begin{aligned}
F_2(x_o^2) &= [(B + C + D)g^2 - Ek^2gh + Ak^4h^2] \\
F_2(y_o^2) &= [(D - B - C)g^2 + Ek^2gh - Ak^4h^2] \\
F_2(x_o'^2) &= [(B + C + D)h^2 + Egh + Ag^2] \\
F_2(y_o'^2) &= [(D - B - C)h^2 - Egh - Ag^2] \\
F_2(x_ox_o') &= [2(B + C + D)gh + E(g^2 - k^2h^2) - 2Ak^2gh] \\
F_2(y_oy_o') &= [2(D - B - C)gh - E(g^2 - k^2h^2) + 2Ak^2gh] \\
F_2(x_o\delta) &= [2(B + C + D)gd + E(fgh - k^2dh) \\
&\qquad - 2k^2Afh^2 + (F + G)g] \\
F_2(x_o'\delta) &= [2(B + C + D)hd + E(fh^2 + gd) \\
&\qquad + 2Afgh + (F + G)h] \\
F_2(\delta^2) &= [(B + C + D)d^2 + Edfh + (F + G)d + H].
\end{aligned}
\tag{34}
$$

y-Forcing Functions:

$$
\begin{aligned}
F_2(x_oy_o) &= [2(B - C)g^2 - 2k^2Egh + 2Ak^4h^2] \\
F_2(x_o'y_o') &= [2(B - C)h^2 + 2Egh + 2Ag^2] \\
F_2(x_oy_o') &= [2(B - C)gh + E(g^2 - k^2h^2) - 2Ak^2gh] \\
F_2(x_o'y_o) &= [2(B - C)gh + E(g^2 - k^2h^2) - 2Ak^2gh] \\
F_2(y_o\delta) &= [2(B - C - D)gd + E(fgh - k^2dh) \\
&\qquad - 2Ak^2fh^2 + (F - G)g] \\
F_2(y_o'\delta) &= [2(B - C - D)hd + E(fh^2 + gd) \\
&\qquad + 2Afgh + (F - G)h].
\end{aligned}
\tag{35}
$$

The notation can be greatly simplified by writing the expressions for the electric and magnetic fields in the magnetic midplane (the dispersion plane, $y = 0$) as follows,

$$\begin{aligned} B_y(x,0,z) &= B_1 + 2B_2x + 3B_3x^2 + \cdots \\ &= B_1\left[1 + 2b_2\frac{x}{R_o} + 3b_3\frac{x^2}{R_o^2} + \cdots\right] \\ E_x(x,0,z) &= E_1 + 2E_2x + 3E_3x^2 + \cdots \\ &= E_1\left[1 + 2e_2\frac{x}{R_o} + 3e_3\frac{x^2}{R_o^2} + \cdots\right]. \end{aligned} \tag{36}$$

Note that the constants b_i and e_i are dimensionless. The forcing function coefficients in equation (31) can now be more simply represented in terms of the cyclotron radius and the expansion coefficients for the fields b_2, b_3, e_2 and e_3. Necessary combinations of these coefficients for determining the second order transfer matrix elements are

$$\begin{aligned} C_1 &= A = \frac{1}{2R_o} \\ C_2 &= B + C + D = -\frac{1}{R_o^3}\left[3(e_3 - b_3) + (5e_2 - 2b_2) + \frac{5}{2}\right] \\ C_3 &= D - B - C = -\frac{1}{R_o^3}\left[3(b_3 - e_3) - e_2\right] \\ C_4 &= F + G = -\frac{1}{R_o^2}\left[(b_2 - 2e_2) - \frac{5}{2}\right] \\ C_5 &= F - G = -\frac{1}{R_o^2}\left[2e_2 - b_2\right] \\ C_6 &= H = -\frac{5}{8R_o} \\ C_7 &= B - C = -\frac{1}{R_o^3}\left[3(b_3 - e_3) + (b_2 - 2e_2)\right] \\ C_8 &= B - C - D = -\frac{1}{R_o^3}\left[3(b_3 - e_3) + 2(b_2 - 2e_2) - \frac{5}{4}\right]. \end{aligned} \tag{37}$$

The matrix elements given in equations (25) and (26) can be defined in terms of these new coefficients and some characteristic integrals given in Appendix 1. Explicit expressions for the matrix elements are given below ($f = 1/2R_o$ and $k = 1/\sqrt{2}R_o$).

x-Aberration Matrix Elements:

$$\begin{aligned} (x\,|\,x_o^2) &= C_2I_{11} + k^4C_1I_{22} \\ (x\,|\,y_o^2) &= C_3I_{11} - k^4C_1I_{22} \\ (x\,|\,x_o'^2) &= C_2I_{22} + C_1I_{11} \\ (x\,|\,y_o'^2) &= C_3I_{22} - C_1I_{11} \\ (x\,|\,x_ox_o') &= 2C_2I_{12} - 2k^2C_1I_{12} \\ (x\,|\,y_oy_o') &= 2C_3I_{12} + 2k^2C_1I_{12} \\ (x\,|\,x_o\delta) &= 2C_2I_{13} - 2k^2fC_1I_{22} + C_4I_1 \\ (x\,|\,x_o'\delta) &= 2C_2I_{23} + 2fC_1I_{12} + C_4I_2 \\ (x\,|\,\delta^2) &= C_2I_{33} + C_4I_3 + C_6I_0. \end{aligned} \tag{38}$$

y-Aberration Matrix Elements:

$$\begin{aligned} (y\,|\,x_oy_o) &= 2C_7I_{11} + 2k^4C_1I_{22} \\ (y\,|\,x_o'y_o') &= 2C_7I_{22} + 2C_1I_{11} \\ (y\,|\,x_oy_o') &= 2C_7I_{12} - 2k^2C_1I_{12} \\ (y\,|\,x_o'y_o) &= 2C_7I_{12} - 2k^2C_1I_{12} \\ (y\,|\,y_o\delta) &= 2C_8I_{13} - 2k^2fC_1I_{22} + C_5I_1 \\ (y\,|\,y_o'\delta) &= 2C_8I_{23} + 2fC_1I_{12} + C_5I_2. \end{aligned} \tag{39}$$

x'-Aberration Matrix Elements:

$$\begin{aligned} (x'\,|\,x_o^2) &= C_2I'_{11} + k^4C_1I'_{22} \\ (x'\,|\,y_o^2) &= C_3I'_{11} - k^4C_1I'_{22} \\ (x'\,|\,x_o'^2) &= C_2I'_{22} + C_1I'_{11} \\ (x'\,|\,y_o'^2) &= C_3I'_{22} - C_1I'_{11} \\ (x'\,|\,x_ox_o') &= 2C_2I'_{12} - 2k^2C_1I'_{12} \\ (x'\,|\,y_oy_o') &= 2C_3I'_{12} + 2k^2C_1I'_{12} \\ (x'\,|\,x_o\delta) &= 2C_2I'_{13} - 2k^2fC_1I'_{22} + C_4I'_1 \\ (x'\,|\,x_o'\delta) &= 2C_2I'_{23} + 2fC_1I'_{12} + C_4I'_2 \\ (x'\,|\,\delta^2) &= C_2I'_{33} + C_4I'_3 + C_6I'_0. \end{aligned} \tag{40}$$

y'-Aberration Matrix Elements:

$$\begin{aligned} (y'\,|\,x_oy_o) &= 2C_7I'_{11} + 2k^4C_1I'_{22} \\ (y'\,|\,x_o'y_o') &= 2C_7I'_{22} + 2C_1I'_{11} \\ (y'\,|\,x_oy_o') &= 2C_7I'_{12} - 2k^2C_1I'_{12} \\ (y'\,|\,x_o'y_o) &= 2C_7I'_{12} - 2k^2C_1I'_{12} \\ (y'\,|\,y_o\delta) &= 2C_8I'_{13} - 2k^2fC_1I'_{22} + C_5I'_1 \\ (y'\,|\,y_o'\delta) &= 2C_8I'_{23} + 2fC_1I'_{12} + C_5I'_2. \end{aligned} \tag{41}$$

6. Fringing fields

In order to calculate the properties of the fringe fields, we need to form expressions for the fields including the z-dependence at the boundaries. Since both electric and magnetic fields are derived from scalar potentials, we can rewrite expressions for the fringe fields from equations (14–17) including the effects of curved (but not tilted) pole face boundaries [22, 23, 32]. Pole boundaries which are not tilted are defined such that the normal to the pole face is parallel to the central ray trajectory as shown in fig. 2.

Define R_m and R_e, additionally subscripted with (in) and (out) when they represent the entrance and exit sides of the Wien filter respectively, as the radii of curvature for the magnetic and electric pole face boundaries. Positive radii have the center of curvature situated on the filter side of the boundary as illustrated in fig. 2. To extract the fringe field matrix elements, the second order trajectory equation is written in time dependent form and integrated directly. The integral equations can be solved by successive approximation and the transfer matrix elements for the fringe fields to second order in the dispersion direction and to first order in the direction perpendicular to the dispersion plane are repeated here [22, 23]. Unspecified matrix elements are zero.

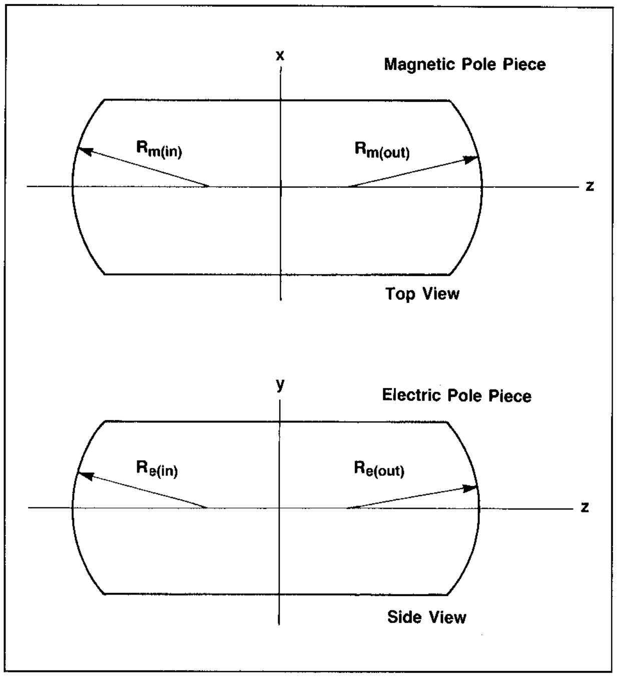

Fig. 2. The curved pole face boundaries for the magnetic (top) and electric (bottom) pole faces. Positive radii of curvature have the center of curvature within the filter as shown.

Entrance-Face Fringe Field

$$\begin{aligned}
&(x \mid x_o) = 1 - \frac{I_1}{x_o}\\
&(x \mid x_o^2) = -\frac{1}{2R_o}\\
&(x \mid y_o^2) = \frac{1}{2R_o}\\
&(x' \mid x_o) = -I_2\\
&(x' \mid x_o') = 1\\
&(x' \mid x_o^2) = \frac{1}{2R_o}\left[\frac{1}{R_{m(\mathrm{in})}} + \frac{1}{R_{e(\mathrm{in})}}\right]\\
&(x' \mid y_o^2) = -\frac{1}{2R_o}\left[\frac{1}{R_{m(\mathrm{in})}} + \frac{1}{R_{e(\mathrm{in})}}\right]\\
&(y \mid y_o) = 1\\
&(y' \mid y_o') = 1.
\end{aligned} \tag{42}$$

Exit-Face Fringe Field

$$\begin{aligned}
&(x \mid x_o) = 1 + \frac{I_1}{x_o}\\
&(x \mid x_o^2) = \frac{1}{2R_o}\\
&(x \mid y_o^2) = -\frac{1}{2R_o}\\
&(x' \mid x_o) = I_2\\
&(x' \mid x_o') = 1\\
&(x' \mid x_o^2) = \frac{1}{2R_o}\left[\frac{1}{R_{m(\mathrm{in})}} + \frac{1}{R_{e(\mathrm{in})}}\right]\\
&(x' \mid y_o^2) = -\frac{1}{2R_o}\left[\frac{1}{R_{m(\mathrm{in})}} + \frac{1}{R_{e(\mathrm{in})}}\right]\\
&(y \mid y_o) = 1\\
&(y' \mid y_o') = 1.
\end{aligned} \tag{43}$$

The integrals I_1 and I_2 are characteristic of the details of the fringing fields. The fringing field integrals are given in terms of $h_m(z)$ and $h_e(z)$ where $B(0,0,z) = B_1\, h_m(z)$ and $E(0,0,z) = E_1\, h_e(z)$. The functions $h_m(z)$ and $h_e(z)$ contain all of the z dependence of the midplane fields. These functions are shown schematically in fig. 3. The functional form of $h_m(z)$ and $h_e(z)$ will depend on the details of the electrode/pole piece construction at the filter boundaries. Additionally shown in fig. 3 is the definition of the effective length of the Wien filter. It is determined such that a *SCOFF* field of length L has the same integrated area ($\int E\,dz$ or $\int B\,dz$) as the real field. The effective pole boundaries need not coincide with the mechanical pole boundaries. The integrals I_1 and I_2 are given below

$$I_1 = \frac{1}{R_o} \int_{za}^{zb} dz \int_{za}^{z} dz\,[h_e(z) - h_m(z)], \tag{44}$$

$$I_2 = \frac{1}{R_o^2} \int_{za}^{zb} dz\, h_e(z)\,[h_m(z) - h_e(z)]. \tag{45}$$

The effective edges of both the electric and magnetic fields are assumed to be aligned for the above cases. The limits on the integrals are selected such that the entire fringe field region lies in the interval $za < z < zb$ for both the entrance and exit fringe fields. In other words, for the entrance pole face boundary, za lies in the field free region and zb lies in the uniform field region. Note that if one wishes to eliminate the zeroeth order trajectory displacement effect of the fringing fields that the functions $h_e(z)$ and $h_m(z)$ must be equal. This corresponds to a situation where the electric and magnetic fringe fields extend with the same functional form [5]. The Wien filter thus has the advantage that the fringe field components can balance each other in the zeroeth order, a situation which does not exist for purely magnetic or electrostatic sectors.

To transport an electron through the Wien filter, the transfer matrices of both entrance and exit fringing fields, entrance and exit drift spaces and Wien filter transfer matrices must be multiplied in the appropriate fashion as [T] = [Drift(out)] [Fringe(out)] [Wien] [Fringe(in)] [Drift(in)] [22, 23, 31, 32, 33, 34].

7. Polarization vector rotation

Experiments involving the detection and measurement of electron-spin require an electron-spin polarimeter. These

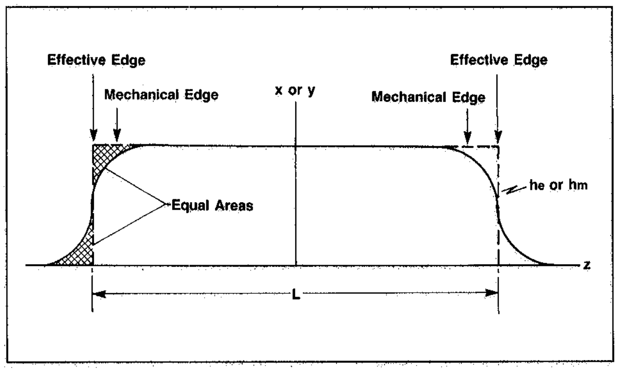

Fig. 3. The fringe fields for the Wien filter as specified by the central ray normalized fields $h_e(z)$ and $h_m(z)$. Also shown are the mechanical pole face boundaries and the effective pole face boundaries. The effective length of the filter in the *SCOFF* approximation is given by the length L.

electron-spin detectors usually consist of a high Z scattering target such as gold and two or more electron counters. The spin separation occurs as a result of the spin-orbit scattering asymmetry. Electrons will be preferentially scattered towards either the left or right side of the detector depending upon the spin orientation of the electron. By having two (or more) [35, 36, 37] particle counters placed symmetrically about the target normal (electron axis), the electron-spin polarization may be measured. These detectors are only sensitive to components of the polarization vector which lie in the plane of the scattering target. If a component of the polarization lies out of the plane of the detector, the spin must be rotated into the detector plane such that a spin-polarization measurement can be performed.

The electron-spin polarization vector may be rotated in two principal directions. For rotations about the longitudinal component, where the longitudinal component is that component of the polarization vector directed along the electron's trajectory, an axially symmetric magnetic field aligned along the electron motion may be used. In the axially symmetric magnetic field the transverse components precess about the magnetic field, while the longitudinal component remains fixed. For rotations about one of the transverse components, we require a magnetic field in the transverse direction, or we must deflect the particle and not rotate its spin. There are several electron-optical devices which perform this function.

For low energies, an electrostatic deflector of 90° bending angle will deflect the electron trajectories by 90° while leaving the orientation of the spin fixed. In this case we are altering the longitudinal direction relative to the spin such that the electron as it exists the deflector has the desired component (initially longitudinal to the trajectory) of the polarization transverse to the trajectory. In a uniform or inhomogeneous field Wien filter, a transverse magnetic field is used to precess the spin, while an electric field maintains the orientation of the particle trajectory. Here, the spin direction precesses relative to the trajectory direction in order for the initially longitudinal component of the spin to become transverse.

In the conventional development of electron-spin rotation in electron optical devices, only the lowest order effects are considered [11, 13]. In the usual treatment, off-axis components of the fields and the differences in path lengths due to different trajectories are not considered. We will begin by using the conventional methodology to estimate the spin precession in an inhomogeneous field Wien filter and later we will expand the approach to include higher order corrections.

The precession of longitudinal to transverse spin in the uniform field Wien filter for the central ray trajectory is characterized by the angle φ of rotation (the longitudinal direction corresponds to the z direction). This rotation angle is given by [11, 13]

$$\varphi = \int_0^L \frac{\eta B_1}{v}\, dz = \frac{\eta B_1 L}{v} \tag{46}$$

where L is the effective length of the *SCOFF* field of the Wien filter. B_1 is the value of the magnetic field along the primary ray in the uniform field Wien filter. Let an arbitrary polarization vector $\boldsymbol{P}$ be expressed as $\boldsymbol{P} = P_{xo}\hat{x} + P_{yo}\hat{y} + P_{zo}\hat{z}$ and let the axis of the magnetic field of the Wien filter be positioned such that it lies at some angle ϑ to the $\hat{y}$ axis where positive ϑ is measured as shown in fig. 4. The magnetic axis orientation of the Wien filter in the frame of the original polarization axes is $\hat{b} = \boldsymbol{B}/B = -\hat{x}\sin\vartheta + \hat{y}\cos\vartheta$. This defines a new coordinate system $(\hat{e}_1, \hat{e}_2, \hat{e}_3)$ such that the magnetic field lies along $\hat{e}_2$. The new coordinate system will be useful in determining the spin rotation for Wien filters whose fields are not perfectly aligned with the initial polarization axes. The new coordinate system in the original polarization vector frame as pictured in fig. 4 is given by

$$\hat{e}_1 = \hat{x}\cos\vartheta + \hat{y}\sin\vartheta \quad \hat{e}_2 = \hat{b} = -\hat{x}\sin\vartheta + \hat{y}\cos\vartheta$$
$$\hat{e}_3 = \hat{z}. \tag{47}$$

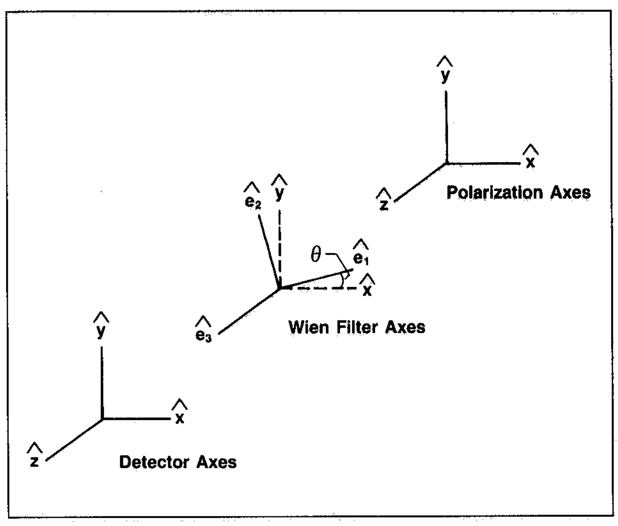

Fig. 4. The axes orientation for initial polarization, the tilted uniform field Wien filter and the electron-spin polarization detector used to estimate the upper limit on the error of spin rotation due to the inhomogeneous fields in the double focusing Wien filter.

In the coordinate system of the Wien filter, the polarization vector is

$$\boldsymbol{P} = (P_{xo} \cos \vartheta + P_{yo} \sin \vartheta)\hat{e}_1 + (P_{yo} \cos \vartheta - P_{xo} \sin \vartheta)\hat{e}_2 + P_{zo}\hat{e}_3 \qquad (48)$$

and the precession of $\boldsymbol{P}$ about the $\hat{e}_2$ (uniform magnetic field) axis by some angle φ is governed by the following transformation

$$\boldsymbol{P}(\varphi) = \begin{bmatrix} \cos\varphi & 0 & \sin\varphi \\ 0 & 1 & 0 \\ -\sin\varphi & 0 & \cos\varphi \end{bmatrix} \cdot \boldsymbol{P}(0)$$
$$= \hat{e}_1 [(P_{xo} \cos \vartheta + P_{yo} \sin \vartheta) \cos \varphi + P_{zo} \sin \varphi] + \hat{e}_2 [P_{yo} \cos \vartheta - P_{xo} \sin \vartheta] + \hat{e}_3 [-(P_{xo} \cos \vartheta + P_{yo} \sin \vartheta) \sin \varphi + P_{zo} \cos \varphi]. \qquad (49)$$

The detector [35, 36, 37] which separates spins via the spin-orbit interaction measures the transverse components of the polarization. Assuming that the detector axes are aligned with the initial $\hat{x}$ and $\hat{y}$ polarization axes, as in fig. 4, the measured components of the polarization vector are

$$\boldsymbol{P} \cdot \hat{x} = P_{xo}(\cos^2 \vartheta \cos \varphi + \sin^2 \vartheta) + P_{yo} \sin \vartheta \cos \vartheta (\cos \varphi - 1) + P_{zo} \cos \vartheta \sin \varphi$$
$$\boldsymbol{P} \cdot \hat{y} = P_{xo} \sin \vartheta \cos \vartheta (\cos \varphi - 1) + P_{yo}(\sin^2 \vartheta \cos \varphi + \cos^2 \vartheta) + P_{zo} \sin \vartheta \sin \varphi. \qquad (50)$$

Beerlage and Farago [13] use this approach of tilted Wien filter fields to perform polarization measurements on all spin components when only one particular polarization direction can be detected in the analyzer. We can use this simple transformation to estimate the degree of mixing of the polarizations due to the tilt of the fields in the stigmatic focusing Wien filter. In this particular case, we can model the magnetic field as follows:

$$\boldsymbol{B} = B_o \left[\left(1 - \frac{y}{2R_o} \right) \hat{y} - \frac{x}{2R_o} \hat{x} \right]. \qquad (51)$$

The tilt angle ϑ is given in the worst case by the following expression

$$\tan \vartheta = \frac{x_{\max}/2R_o}{1 - y_{\max}/2R_o}. \qquad (52)$$

Reasonable electric and magnetic fields are required for spin rotation of a 1 keV electron beam. Assuming the maximum displacements $x_{\max}$ and $y_{\max}$ of the beam trajectory of 2 mm, we can estimate the upper limit on the error induced in $\boldsymbol{P}$ after the spin rotation for pure longitudinal to transverse rotations of $\pi/2$ ($P_z \to P_x$) by looking at the residual polarization in $\hat{y}$ as a result of the $\hat{x}$-component of the magnetic field. As a function of the cyclotron radius these estimates are given in the table 1 below.

Table 1. Estimate of polarization mixing due to tilted fields in the Wien filter.

R_o(mm)	ϑ	P_y
50	1.16°	0.02
20	3.01°	0.05
10	6.33°	0.11

7.1. Equation of motion for electron spins in an inhomogeneous field Wien filter

The estimation of the spin precession given above is for purely homogeneous fields. In that case the spin precesses about the magnetic field vector at a fixed rate. In the integral expression for the rotation angle φ, no account was taken of field inhomogeneities, or the difference between particular electron trajectory lengths through the filter. In order to correctly incorporate these considerations, we will derive a spin-rotation matrix which will relate the initial electron position, slope and polarization to that which will be found at the output of the filter. We will derive the coupled equations of motion for the spins in the Wien filter, and parameterize the spin-trajectories and thereby the fields in terms of the matrix elements for the spatial variables which were derived in the previous section.

The coupled differential equations governing spin precession about a magnetic field cannot be completely decoupled. In the limit that the rotations are infinitesimal, the rotations can be treated as vectors and thus be decoupled, but if any of the rotations are finite, the rotation operators do not commute and they cannot be separated and treated as vectors [38]. For the same reason, we cannot transform into a rotating coordinate system to simplify the problem [39]. Since the finite rotation regime is the regime in which the Wien filter operates, we cannot separate the individual rotations into components to simplify this problem. We begin the analysis with the time dependent differential equation for spin precession.

The non-relativistic time evolution of the electric spin-polarization vector is governed by the following coupled differential equations [11]

$$\frac{d\boldsymbol{P}}{dt} = -\boldsymbol{\omega}_o \times \boldsymbol{P} \quad \boldsymbol{\omega}_o = \frac{eg\boldsymbol{B}}{2m} = -\frac{g\eta\boldsymbol{B}}{2}. \qquad (53)$$

g is the electron gyromagnetic ratio. The value of $g = 2.00116$ [35]. This means that for each cyclotron orbit, that the phase of the spin and the orbit is shifted by 0.1 percent. We will assume here that $g = 2$ since our Wien filter will not rotate the spins by more than a couple of orbits thereby introducing an error of less than 0.2 percent. The time dependent spin equation must be parameterized in terms of the coordinate z, and all field quantities must be expanded into series. We will be able to derive a formalism similar to that developed for the spatial trajectories in this way. We find the spin equation equivalent of the spatial trajectory equation given by equation (18)

$$\frac{d\boldsymbol{P}}{dz} = \sqrt{\frac{\eta}{2\phi}} \sqrt{1 + x'^2 + y'^2}\, \boldsymbol{B} \times \boldsymbol{P}. \qquad (54)$$

We make the simplifying assumption, applicable here, that the magnetic field in the z direction will be zero (*SCOFF* approximation). This is not unreasonable in the sense that the z-directed field exists only in the fringe field regions and thus we expect the perturbation due to these fields to be small. We can justify this easily in the limit that the Wien filter length-to-gap ratio is large. However, considering the z component of the fringe field to be of the same order as the transverse field inhomogeneities within the Wien filter's main fields, it is immediately evident that the fringe field components are negligible. Since the integral of $\boldsymbol{B}$ is taken over path lengths which are much shorter for passage through the fringing field region than passage through the main fields, we will neglect the fringe field inhomogneities for electron-spin precession.

The z-dependent spin-precession equations (54) can be combined to form two second order and one first order equation which will be the starting point for our analysis

$$\frac{d^2 P_x}{dz^2} = P_z \frac{d}{dz}\left[\sqrt{\frac{\eta}{2\phi}}\sqrt{1+x'^2+y'^2}\,B_y\right] + \frac{\eta}{2\phi}(1+x'^2+y'^2)\,[P_y B_x B_y - P_x B_y^2], \quad (55)$$

$$\frac{dP_y}{dz} = -\sqrt{\frac{\eta}{2\phi}}\sqrt{1+x'^2+y'^2}\,B_x P_z, \quad (56)$$

$$\frac{d^2 P_z}{dz^2} = P_y \frac{d}{dz}\left[\sqrt{\frac{\eta}{2\phi}}\sqrt{1+x'^2+y'^2}\,B_x\right] - P_x \frac{d}{dz}\left[\sqrt{\frac{\eta}{2\phi}}\sqrt{1+x'^2+y'^2}\,B_y\right] - \frac{\eta}{2\phi}(1+x'^2+y'^2)\,[P_z B_x^2 + P_z B_y^2]. \quad (57)$$

Evaluating the derivatives to second order and making the appropriate substitutions for the potential and the fields, we find the second order spin-precession equations

$$\begin{aligned}\frac{d^2 P_x}{dz^2} + \frac{P_x}{R_o^2} = &-\frac{P_x}{R_o^2}\Bigg[2(2b_2+1)\frac{x}{R_o} - \delta + x'^2 + y'^2 \\ &+ 2[3b_3 + 2b_2(b_2+2) + e_2 + 2]\frac{x^2}{R_o^2} \\ &- 2(3b_3+e_2)\frac{y^2}{R_o^2} + \delta^2 - 4(b_2+1)\frac{x\delta}{R_o}\Bigg] \\ &+ \frac{P_y}{R_o^2}\left[2b_2\frac{y}{R_o} + 2[3b_3 + 2b_2(b_2+1)]\frac{xy}{R_o^2} - 2b_2\frac{y\delta}{R_o}\right] \\ &+ \frac{P_z}{R_o^2}\Bigg[(2b_2+1)x' + 2(3b_3+3b_2+1)\frac{xx'}{R_o} \\ &- 2(3b_3+b_2)\frac{yy'}{R_o} - (b_2+1)x'\delta\Bigg], \end{aligned} \quad (58)$$

$$\frac{dP_y}{dz} = -\frac{P_z}{R_o}\left[2b_2\frac{y}{R_o} + 2(3b_3+b_2)\frac{xy}{R_o} - b_2\frac{y\delta}{R_o}\right], \quad (59)$$

$$\begin{aligned}\frac{d^2 P_z}{dz^2} + \frac{P_z}{R_o^2} = &-\frac{P_x}{R_o^2}\Bigg[(2b_2+1)x' + 2(3b_3+3b_2+1)\frac{xx'}{R_o} \\ &- 2(3b_3+b_2)\frac{yy'}{R_o} - (b_2+1)x'\delta\Bigg] \\ &+ \frac{P_y}{R_o^2}\left[2b_2 y' + 2(3b_3+b_2)\frac{xy'+x'y}{R_o} - b_2 y'\delta\right] \\ &- \frac{P_z}{R_o^2}\Bigg[2(2b_2+1)\frac{x}{R_o} - \delta \\ &+ 2[3b_3 + 2b_2(b_2+2) + e_2 + 2]\frac{x^2}{R_o^2}\Bigg] + x'^2 + y'^2 \\ &- 2(3b_3 - 2b_2^2 + e_2)\frac{y^2}{R_o^2} + \delta^2 - 4(b_2+1)\frac{x\delta}{R_o}\Bigg]. \end{aligned} \quad (60)$$

In order to solve these equations, we make the same assumptions that were successfully implemented in the spatial trajectory calculations, namely expand the electron-spin polarization components into Taylor series expansions

$$P_x = \sum (P_x | P_{xo}^i P_{yo}^j P_{zo}^k x_o^l x_o'^m y_o^n y_o'^p \delta^q)\, P_{xo}^i P_{yo}^j P_{zo}^k x_o^l x_o'^m y_o^n y_o'^p \delta^q$$

$$\begin{aligned} P_x = &(P_x|P_{xo})P_{xo} + (P_x|P_{zo})P_{zo} + (P_x|P_{xo}x_o)P_{xo}x_o \\ &+ (P_x|P_{zo}x_o)P_{zo}x_o + (P_x|P_{xo}x_o')P_{xo}x_o' \\ &+ (P_x|P_{zo}x_o')P_{zo}x_o' + (P_x|P_{xo}\delta)P_{xo}\delta + (P_x|P_{zo}\delta)P_{zo}\delta \\ &+ (P_x|P_{yo}y_o)P_{yo}y_o + (P_x|P_{yo}y_o')P_{yo}y_o', \end{aligned} \quad (61)$$

$$P_y = \sum (P_y | P_{xo}^i P_{yo}^j P_{zo}^k x_o^l x_o'^m y_o^n y_o'^p \delta^q)\, P_{xo}^i P_{yo}^j P_{zo}^k x_o^l x_o'^m y_o^n y_o'^p \delta^q$$

$$\begin{aligned} P_y = &(P_y|P_{xo}y_o)P_{xo}y_o + (P_y|P_{zo}y_o)P_{zo}y_o + (P_y|P_{xo}y_o')P_{xo}y_o' \\ &+ (P_y|P_{zo}y_o')P_{zo}y_o', \end{aligned} \quad (62)$$

$$P_z = \sum (P_z | P_{xo}^i P_{yo}^j P_{zo}^k x_o^l x_o'^m y_o^n y_o'^p \delta^q)\, P_{xo}^i P_{yo}^j P_{zo}^k x_o^l x_o'^m y_o^n y_o'^p \delta^q, \quad (63)$$

$$\begin{aligned} P_z = &(P_z|P_{xo})P_{xo} + (P_z|P_{zo})P_{zo} + (P_z|P_{xo}x_o)P_{xo}x_o \\ &+ (P_z|P_{zo}x_o)P_{zo}x_o + (P_z|P_{xo}x_o')P_{xo}x_o' \\ &+ (P_z|P_{zo}x_o')P_{zo}x_o' + (P_z|P_{xo}\delta)P_{xo}\delta + (P_z|P_{zo}\delta)P_{zo}\delta \\ &+ (P_z|P_{yo}y_o)P_{yo}y_o + (P_z|P_{yo}y_o')P_{yo}y_o'. \end{aligned} \quad (64)$$

First consider solving these equations for the first order solutions whereby the spatial variation of the fields and the spatial trajectory variations of the path lengths are ignored. This corresponds to solving the standard polarization rotation equations for rotation about a uniform magnetic field directed in the y direction. These first order solutions are

$$\begin{aligned} P_x &= P_{xo}\cos\left(\frac{z}{R_o}\right) + P_{zo}\sin\left(\frac{z}{R_o}\right), \\ P_y &= P_{yo}, \\ P_z &= P_{zo}\cos\left(\frac{z}{R_o}\right) - P_{xo}\sin\left(\frac{z}{R_o}\right). \end{aligned} \quad (65)$$

The derivatives are

$$\begin{aligned} P_x' &= -\frac{P_{xo}}{R_o}\sin\left(\frac{z}{R_o}\right) + \frac{P_{zo}}{R_o}\cos\left(\frac{z}{R_o}\right) = \frac{P_z}{R_o}, \\ P_y' &= 0, \\ P_z' &= -\frac{P_{zo}}{R_o}\sin\left(\frac{z}{R_o}\right) - \frac{P_{xo}}{R_o}\cos\left(\frac{z}{R_o}\right) = -\frac{P_x}{R_o}. \end{aligned} \quad (66)$$

We can rewrite the solutions to the first order spin trajectory equations in a form compatible with the formalism developed for the spatial trajectories. Consider solutions of the form:

$$P_x = G(z)\,P_{xo} + H(z)\,P'_{xo}, \quad P_y = P_{yo},$$
$$P_z = G(z)\,P_{zo} + H(z)\,P'_{zo}, \tag{67}$$

where the first order solutions to the P_x and P_z equations are

$$G(z) = \cos\left(\frac{z}{R_o}\right), \quad H(z) = R_o \sin\left(\frac{z}{R_o}\right). \tag{68}$$

We can develop expansions for the aberrations (second-order matrix elements) in terms of the forcing functions as described by equation (27) except now the Green's function for x and z spin-precession is

$$G_s(z,\tau) = H(z)\,G(\tau) - G(z)\,H(\tau) = R_o \sin\left[\frac{(z-\tau)}{R_o}\right] \tag{69}$$

and the Green's function for the y spin-precession $G_{sy}(z,\tau) = 1$. We use the notation above for P'_{xo} and P'_{zo} realizing that when the expressions are evaluated that $P'_{xo} = P_{zo}/R_o$ and $P'_{zo} = -P_{xo}/R_o$. It is convenient to use this notation because the formalism is well developed for solutions of this form [31]. To solve for the higher order terms in the spin-precession equations, substitute the expressions for the spatial variables in terms of the expansions (25) and (26), substitute for the expansions for the polarizations (61–64), gather terms and form the spin-precession forcing functions. These forcing function expressions are given below.

P_x-Forcing Functions

$$F_{2px}(P_{xo}x_o) = -\frac{(2b_2+1)}{R_o^3}[2gG - k^2hH],$$
$$F_{2px}(P_{zo}x_o) = -\frac{(2b_2+1)}{R_o^4}[2gH + k^2R_o^2hG],$$
$$F_{2px}(P_{xo}x'_o) = -\frac{(2b_2+1)}{R_o^3}[2hG + gH],$$
$$F_{2px}(P_{zo}x'_o) = -\frac{(2b_2+1)}{R_o^4}[2hH - R_o^2gG],$$
$$F_{2px}(P_{xo}\delta) = -\frac{(2b_2+1)f}{k^2R_o^3}[2G - 2gG + k^2hH] + \frac{G}{R_o^2},$$
$$F_{2px}(P_{xo}\delta) = -\frac{(2b_2+1)f}{k^2R_o^4}[2H - 2gH - k^2R_o^2hG] + \frac{H}{R_o^3},$$
$$F_{2px}(P_{yo}y_o) = \frac{2b_2}{R_o^3}\,g,$$
$$F_{2px}(P_{yo}y'_o) = \frac{2b_2}{R_o^3}\,h. \tag{70}$$

P_y-Forcing Functions

$$F_{2py}(P_{xo}y_o) = \frac{2b_2}{R_o^3}\,gH,$$
$$F_{2py}(P_{zo}y_o) = -\frac{2b_2}{R_o^2}\,gG,$$
$$F_{2py}(P_{xo}y'_o) = \frac{2b_2}{R_o^3}\,hH,$$
$$F_{2py}(P_{zo}y'_o) = -\frac{2b_2}{R_o^2}\,hG. \tag{71}$$

P_z-Forcing Functions

$$F_{2pz}(P_{xo}x_o) = -F_{2px}(P_{zo}x_o),$$
$$F_{2pz}(P_{zo}x_o) = F_{2px}(P_{xo}x_o),$$
$$F_{2pz}(P_{xo}x'_o) = -F_{2px}(P_{zo}x'_o),$$
$$F_{2pz}(P_{zo}x'_o) = F_{2px}(P_{xo}x'_o),$$
$$F_{2pz}(P_{xo}\delta) = -F_{2px}(P_{zo}\delta),$$
$$F_{2pz}(P_{zo}\delta) = F_{2px}(P_{xo}\delta),$$
$$F_{2pz}(P_{yo}y_o) = -\frac{2b_2k^2}{R_o^2}\,h,$$
$$F_{2pz}(P_{yo}y'_o) = \frac{2b_2}{R_o^2}\,g. \tag{72}$$

The higher order expressions (second order in position and slope) have been derived but the expressions are too lengthy to be included here. The final expressions for the matrix elements for the spin precession can now be expressed in terms of the integrals given in Appendix 2. The explicit expressions for the matrix elements are given below.

P_x-Matrix Elements

$$(P_x|P_{xo}) = G(z),$$
$$(P_x|P_{yo}) = 0,$$
$$(P_x|P_{zo}) = \frac{H(z)}{R_o},$$
$$(P_x|P_{xo}x_o) = -\frac{(2b_2+1)}{R_o^3}[2I_{s11} - k^2I_{s22}],$$
$$(P_x|P_{zo}x_o) = -\frac{(2b_2+1)}{R_o^4}[2I_{s12} + k^2R_o^2I_{s21}],$$
$$(P_x|P_{xo}x'_o) = -\frac{(2b_2+1)}{R_o^3}[2I_{s21} - I_{s12}],$$
$$(P_x|P_{zo}x'_o) = -\frac{(2b_2+1)}{R_o^4}[2I_{s22} - R_o^2I_{s11}],$$
$$(P_x|P_{xo}\delta) = -\frac{(2b_2+1)f}{k^2R_o^3}[2I_{s10} - 2I_{s11} + k^2I_{s22}] + \frac{1}{R_o^2}I_{s01},$$
$$(P_x|P_{zo}\delta) = -\frac{(2b_2+1)f}{k^2R_o^4}[2I_{s20} - 2I_{s12} - k^2R_o^2I_{s21}] + \frac{1}{R_o^3}I_{s02},$$
$$(P_x|P_{yo}y_o) = \frac{2b_2}{R_o^3}I_{s10},$$
$$(P_x|P_{yo}y'_o) = \frac{2b_2}{R_o^3}I_{s20}. \tag{73}$$

P_y-Matrix Elements

$$(P_y|P_{xo}) = 0,$$
$$(P_y|P_{yo}) = 1,$$
$$(P_y|P_{zo}) = 0,$$
$$(P_y|P_{xo}y_o) = \frac{2b_2}{R_o^3} I_{sy12},$$
$$(P_y|P_{zo}y_o) = -\frac{2b_2}{R_o^2} I_{sy11},$$
$$(P_y|P_{xo}y'_o) = \frac{2b_2}{R_o^3} I_{sy22},$$
$$(P_y|P_{zo}y'_o) = -\frac{2b_2}{R_o^2} I_{sy21}. \quad (74)$$

P_z-Expressions

$$(P_z|P_{xo}) = -\frac{1}{R_o} H(z),$$
$$(P_z|P_{yo}) = 0,$$
$$(P_z|P_{zo}) = G(z),$$
$$(P_z|P_{xo}x_o) = -(P_x|P_{zo}x_o),$$
$$(P_z|P_{zo}x_o) = (P_x|P_{xo}x_o),$$
$$(P_z|P_{xo}x'_o) = -(P_x|P_{zo}x'_o),$$
$$(P_z|P_{zo}x'_o) = (P_x|P_{xo}x'_o),$$
$$(P_z|P_{xo}\delta) = -(P_x|P_{zo}\delta),$$
$$(P_z|P_{zo}\delta) = (P_x|P_{xo}\delta),$$
$$(P_z|P_{yo}y_o) = -\frac{2b_2k^2}{R_o^2} I_{s20},$$
$$(P_z|P_{yo}y'_o) = \frac{2b_2}{R_o^2} I_{s10}. \quad (75)$$

Now we can abbreviate the elements of the spin matrix such that bracketed quantities include terms which are summed over the initial polarization, for example, the matrix element $[P_x|P_{xo}]$ is formed by summing all terms

$$[P_x|P_{xo}] = (P_x|P_{xo}) + (P_x|P_{xo}x_o)x_o + (P_x|P_{xo}x'_o)x'_o + (P_x|P_{xo}\delta)\delta. \quad (76)$$

The electron-spin rotation matrix in the frame of the Wien filter where the precession is primarily about the y-axis is given below. This matrix can be substituted into the matrix expression given in equation (49) for a correct second order approximation to the spin-rotation

$$\boldsymbol{P}(z) = \begin{bmatrix} [P_x|P_{xo}] & [P_x|P_{yo}] & [P_x|P_{zo}] \\ [P_y|P_{xo}] & [P_y|P_{yo}] & [P_y|P_{zo}] \\ [P_z|P_{xo}] & [P_z|P_{yo}] & [P_z|P_{zo}] \end{bmatrix} \cdot \boldsymbol{P}(0). \quad (77)$$

Now the electron-spin precession has been characterized such that accurate evaluation of the final spin states can be ascertained.

8. Design examples

In the previous sections we have developed the complete second order transfer matrix for general inhomogeneous field Wien filters including electron-spin precession. The matrix elements are given in a second order approximation and dispersion is treated rigorously. We will apply these results to some simple design examples.

8.1. Energy analyzers

The first example will be the design of an electron energy loss spectrometer which is to be interfaced with an electron microscope [27]. Assume that the object position for the Wien filter (entrance slit) lies at the effective edge at the filter entrance. Further, we will select a 180° Wien filter. We consider the Wien filter to act like a magnetic sector, only the trajectories are straight lines; the equations for the Wien filter and a magnetic sector are similar in the first order, and as such we attribute a bending angle Φ to the Wien filter defined as $\Phi = kz$. In other words, a Wien filter of length $z = \sqrt{2}\pi R_o$. The image plane will lie at the effective edge at the exit to the filter (exit slit). Although this example is not practical for implementation in that the object and image points lie within the fringe field regions and the slits would necessarily interfere with the fringe fields, it is a good example for comparison with the theory of Rose [27].

If we ignore the effects of the fringing fields, we find that the spatial magnification $(x|x_o) = -1$ the angular magnification $(x'|x'_o) = -1$ and the dispersion is $(x|\delta) = 2R_o$. We would like to eliminate the aperture aberrations completely, $(x|x_o'^2) = (x|y_o'^2) = 0$ while maintaining the first order Wien focussing condition $e_2 - b_2 + 1/4 = 0$. Taking the expressions for the matrix elements from equation (38), the coefficients from equation (37) and the integrals from Appendix 1, we find we can eliminate the aberrations if the multipole field excitation parameters are

$$e_2 = -1, \quad b_2 = -\tfrac{3}{4}, \quad (e_3 - b_3) = \tfrac{3}{8}. \quad (78)$$

These results are identical to the results given by Rose [27]. Furthermore, if we assume that the electric potential is generated by a cylindrical condenser, as shown in fig. 1a, the potential ($e_2 = -1$) has the following form,

$$\phi = \phi_o\left(1 - \frac{1}{2}\ln\left[\left(\frac{2x}{R} - 1\right)^2 + \left(\frac{2y}{R}\right)^2\right]\right) \quad (79)$$

where $R = -R_o$. The cylindrical electrodes have the center of curvature r_e located at $-R_o/2$ shown schematically in fig. 1. With this electric potential, we find $e_3 = 4/3$ and $b_3 = 23/24$, in complete agreement with the results of Rose [27] (except here the center of curvature is in the opposite direction due to the assumptions of the initial field direction). Magnetic poles and electrostatic electrodes to actualize this configuration are shown by Rose [27] in his paper and details regarding the numerical trimming of the fields is given by Tsuno et al. [5].

We can treat the situation where we do not totally neglect the effect of the fringing fields, and place the object and image in field free regions. We will assume however, that it is possible to balance the electric and magnetic fringe fields such that integrals I_1 and I_2 of equations (44) and (45) are zero.

This eliminates the zeroeth order displacement and first order angular focusing of the fringe fields. Numerical details of this procedure will be given in a subsequent paper. Further, we will constrain the entrance and exit pole face radii to be infinite, i.e. the entrance and exit pole faces shown in fig. 2 are flat. This requirement should facilitate alignment. All other design requirements being the same, the following system of equations must be solved

$$(x\,|\,x_o'^2)_{\text{total}} = -\frac{gd_o^2}{2R_o} + (x\,|\,x_o'^2) + \frac{k^2hd_o^2d_i}{2R_o} + (x'\,|\,x_o'^2)\,d_i + \frac{h^2}{2R_o} = 0,$$

$$(x\,|\,y_o'^2)_{\text{total}} = \frac{gd_o^2}{2R_o} + (x\,|\,y_o'^2) - \frac{k^2hd_o^2d_i}{2R_o} + (x'\,|\,y_o'^2)\,d_i - \frac{h^2}{2R_o} = 0,$$

$$e_2 - b_2 + \frac{1}{4} = 0. \tag{80}$$

g and h are the ray trajectory solutions and d_o and d_i are the object and image side drift distances to the appropriate effective edge of the Wien filter. We will assume that a bending angle of $kz = 5\pi/6 = 150°$ or $z = 5\sqrt{2}\pi/6R_o$ is suitable. We would like the magnification to be unity as above, such that $d_o = d_i = \sqrt{2}(2-\sqrt{3})R_o$. The equations can be solved and we find that $e_2 = -1$, $b_2 = -3/4$ and $e_3 - b_3 = 0.3879$. We can separate the hexapole coefficients as done above to determine the individual multipole field excitations. Numerical ray tracing should be done in order to refine the calculation in the fields near the entrance and exit pole face boundaries [5].

We have shown that using the formalism derived above that we can easily design a second order aperture aberration corrected energy loss spectrometer. Other constraints may be included in the design procedure. One possible auxilliary constraint is the elimination of the image plane tilt aberration $(x\,|\,x_o'\delta)$ such that the image (dispersion) plane is normal to the electron trajectories. The requirement will facilitate the implementation of parallel recording for the acquisition of spectra.

8.2. Spin-rotators

We could begin this design by selecting an aberration corrected electron energy analyzer as above, choose the length to perform the desired spin rotation and then determine the effect that the fields have on perturbing the ideal electron-spin rotation. Instead, we will concentrate on a specific example of an electron-spin rotator disregarding the device's properties as an energy analyzer.

For the design of an electron-spin rotator, the usual requirement is to precess the spin from a longitudinal (spin pointing along $\boldsymbol{v}$ = velocity vector) orientation to a transverse orientation. This is a requirement because most electron-spin polarimeters are sensitive to transverse components of spin only [35, 36, 37]. The easiest solution to elimiante any precession into P_y is to align the Wien filter magnetic field with the y-polarization axis, and choose the quadrupole excitation parameters $b_2 = 0$ and $e_2 = 1/4$. This selection guarantees that all P_y terms in the spin-rotation matrix are zero and that the Wien filter is double focusing. To continue to correct for the spin-rotation aberrations, consider the situation where the object position is at the entrance to the Wien filter. We would thus like to eliminate terms containing slopes such as $(P_x\,|\,P_{xo}x_o')$ since these will be the dominant terms. In order to do this, the length of the Wien filter must be carefully selected such that $I_{s12} + 2I_{s21} = 0$ and $2I_{s22} - R_o^2 I_{s11} = 0$, where the integrals are defined in Appendix 2. The first order solution to the Wien filter equation for longitudinal to transverse $((2n+1)\,\pi/2)$ rotations must have $G(z) = 0$ and $H(z) = \pm 1$. To eliminate the sums of the integrals cited above, $g(z) = 0$. This means that

$$Kz = kz = \frac{(2n+1)\,\pi}{2} \tag{81}$$

where n is an integer. The first occurance which closely approximates this condition is $Kz = 7\pi/2$, which forces $kz = 4.95\pi/2$. To first order, the spin precesses by 1 3/4 complete rotations. The periodicity of the Wien filter orbit almost completes 1 1/4 complete rotations. The maximum error in the spin due to aberrations will be about $0.07x_o'$ which is an error of less than 0.01 for entrance angles up to 8.5°. Since kz does not precisely equal $5\pi/2$, the electrons do not emerge exactly parallel from the filter. However, for this example, the error will be less than 0.5°.

The design possibilities for simultaneous energy analysis and spin rotation are endless. The possibility exists, using the formalism developed above to design accurate energy analyzers and spin rotators.

9. Conclusion

The second order transfer matrices for an inhomogeneous field Wien filter have been derived for both the electron trajectories and the electron-spin precession. The formalism developed greatly facilitates the design of precise electron-spin rotators which may be used in experiments with polarized electrons, electron energy loss spectrometers and mass filters. For experiments where both spin-rotation and energy analysis is required, this device permits both functions to be performed simultaneously. Furthermore, since the inhomogeneous field Wien filter is stigmatic, it may be incorporated into a beam transport system possessing cylindrical symmetry without disturbing the symmetry of the beam line optics (neglecting dispersion). If the electric and magnetic fringe field effective edges can be aligned, and if the functional form for the fall off of the fringe fields can be made identical for both fringe fields, then the zeroeth order beam displacement and first order beam tilt due to the fringe fields can be eliminated. Finally, examples were given for specific designs whereby aberrations could be eliminated.

Appendix 1: Trajectory forcing function integrals

The general expressions for the forcing function integrals are given below where the following abbreviations are used [31]

$$k^2 = \frac{\eta B_1^2}{4\phi_o} = \frac{E_1^2}{8\phi_o^2} = \frac{1}{2R_o^2}, \; f = \frac{1}{2R_o} = \frac{k}{\sqrt{2}},$$

$$g(z) = \cos(kz),\; h(z) = \frac{1}{k}\sin(kz),\; d(z) = \frac{f}{k^2}(1-\cos(kz)).$$

The general form for the integrals which are required for the determination of the aberration coefficients is given in equation (27). Substituting the expressions for $g(z)$ and $h(z)$ in the *SCOFF* approximation into equation (27) we find

$$\omega_f = \frac{\sin(kz)}{k}\int_0^z f(\tau)\cos(k\tau)\,dt - \frac{\cos(kz)}{k}\int_0^z f(\tau)\sin(k\tau)\,d\tau$$

which reduces to

$$\omega_f = \int_0^z f(\tau)\,G(z,\tau)\,d\tau \quad \text{where} \quad G(z,\tau) = \frac{1}{k}\sin[k(z-\tau)].$$

Explicit expressions for the integrals are given below

$$I_0 = \int_0^z G(z,\tau)\,d\tau = \frac{1}{f}d(z),$$

$$I_1 = \int_0^z g(\tau)\,G(z,\tau)\,d\tau = \frac{z}{2}h(z),$$

$$I_2 = \int_0^z h(\tau)\,G(z,\tau)\,d\tau = \frac{1}{2k^2}[h(z) - zg(z)],$$

$$I_3 = \int_0^z d(\tau)\,G(z,\tau)\,d\tau = \frac{1}{k^2}\left[d(z) - \frac{fz}{2}h(z)\right],$$

$$I_{11} = \int_0^z g^2(\tau)\,G(z,\tau)\,d\tau = \frac{1}{3}\left[h^2(z) + \frac{1}{f}d(z)\right],$$

$$I_{12} = \int_0^z g(\tau)\,h(\tau)\,G(z,\tau)\,d\tau = \frac{1}{3f}h(z)\,d(z),$$

$$I_{13} = \int_0^z g(\tau)\,d(\tau)\,G(z,\tau)\,d\tau = \frac{f}{k^2}[I_1 - I_{11}] = \frac{f}{k^2}\left[\frac{z}{2}h(z) - \frac{1}{3f}[fh^2(z) + d(z)]\right],$$

$$I_{22} = \int_0^z h^2(\tau)\,G(z,\tau)\,d\tau = \frac{1}{k^2}[I_0 - I_{11}] = \frac{1}{3k^2 f}[2d(z) - fh^2(z)],$$

$$I_{23} = \int_0^z h(\tau)\,d(\tau)\,G(z,\tau)\,d\tau = \frac{f}{k^2}[I_2 - I_{12}] = \frac{f}{6k^4}[h(z) + 2h(z)\,g(z) - 3zg(z)],$$

$$I_{33} = \int_0^z d^2(\tau)\,G(z,\tau)\,d\tau = \frac{f^2}{k^4}[I_0 - 2I_1 + I_{11}] = \frac{f^2}{k^4}\left[\frac{4}{3f}d(z) + \frac{1}{3}h^2(z) - zh(z)\right],$$

$$I_0' = \frac{d}{dz}\int_0^z G(z,\tau)\,d\tau = h(z),$$

$$I_1' = \frac{d}{dz}\int_0^z g(\tau)\,G(z,\tau)\,d\tau = \frac{1}{2}[h(z) + zg(z)],$$

$$I_2' = \frac{d}{dz}\int_0^z h(\tau)\,G(z,\tau)\,d\tau = \frac{1}{2}zh(z),$$

$$I_3' = \frac{d}{dz}\int_0^z d(\tau)\,G(z,\tau)\,d\tau = \frac{f}{2k^2}[h(z) - zg(z)],$$

$$I_{11}' = \frac{d}{dz}\int_0^z g^2(\tau)\,G(z,\tau)\,d\tau = \frac{1}{3}[h(z) + 2g(z)\,h(z)],$$

$$I_{12}' = \frac{d}{dz}\int_0^z g(\tau)\,h(\tau)\,G(z,\tau)\,d\tau = \frac{1}{3}\left[2h^2(z) - \frac{1}{f}d(z)\right],$$

$$I_{13}' = \frac{d}{dz}\int_0^z g(\tau)\,d(\tau)\,G(z,\tau)\,d\tau = \frac{f}{k^2}\left[\frac{z}{2}g(z) + \frac{1}{6}h(z) - \frac{2}{3}g(z)\,h(z)\right],$$

$$I_{22}' = \frac{d}{dz}\int_0^z h^2(\tau)\,G(z,\tau)\,d\tau = \frac{2}{3f}h(z)\,d(z),$$

$$I_{23}' = \frac{d}{dz}\int_0^z h(\tau)\,d(\tau)\,G(z,\tau)\,d\tau = \frac{f}{k^2}\left[\frac{z}{2}h(z) - \frac{2}{3}h^2(z) + \frac{1}{3f}d(z)\right],$$

$$I_{33}' = \frac{d}{dz}\int_0^z d^2(\tau)\,G(z,\tau)\,d\tau = \frac{f^2}{k^4}\left[\frac{1}{3}h(z) + \frac{2}{3}h(z)\,g(z) - zg(z)\right].$$

Appendix 2: Spin forcing function integrals

We use the same notation as defined in Appendix 1, with the spin solutions to the differential equations being defined below

$$K^2 = \frac{\eta B_1^2}{2\phi_o} = \frac{E_1^2}{4\phi_o^2} = \frac{1}{R_o^2},$$

$$G(z) = \cos(Kz), \quad H(z) = \frac{1}{K}\sin(Kz).$$

The general form for the integrals which are required for the determination of the x and z spin-precession aberration coefficients is

$$\omega_{F(\mathrm{spin})} = H(z)\int_0^z F_{\mathrm{spin}}(\tau)\,G(\tau)\,d\tau - G(z)\int_0^z F_{\mathrm{spin}}(\tau)\,H(\tau)\,d\tau.$$

Substituting the expressions for $G(z)$ and $H(z)$ we find

$$\omega_{F(\mathrm{spin})} = \int_0^z F_{\mathrm{spin}}(\tau)\,G_s(z,\tau)\,d\tau$$

where

$$G_s(z,\tau) = \frac{1}{K}\sin[K(z-\tau)].$$

The Green's function for the y spin-precession terms is 1. Explicit expressions for the integrals are given below

$$I_{s01} = \int_0^z G(\tau)\, G_s(z,\tau)\,d\tau = \frac{z}{2}H(z),$$

$$I_{s02} = \int_0^z H(\tau)\, G_s(z,\tau)\,d\tau = \frac{1}{2K^2}[H(z) - zG(z)],$$

$$I_{s10} = \int_0^z g(\tau)\, G_s(z,\tau)\,d\tau = \frac{1}{k^2 - K^2}[G(z) - g(z)],$$

$$I_{s20} = \int_0^z h(\tau)\, G_s(z,\tau)\,d\tau = \frac{1}{k^2 - K^2}[H(z) - h(z)],$$

$$I_{s11} = \int_0^z g(\tau)\, G(\tau)\, G_s(z,\tau)\,d\tau$$

$$= \frac{1}{k^2 - 4K^2}[G(z)(1 - g(z)) - 2K^2 H(z)\, h(z)],$$

$$I_{s21} = \int_0^z h(\tau)\, G(\tau)\, G_s(z,\tau)\,d\tau = \frac{1}{k^2 - 4K^2}$$

$$\cdot\left[2\left(\frac{K}{k}\right)^2 H(z)(1 + g(z)) - h(z)\, G(z)\right] + \frac{H(z)}{k^2},$$

$$I_{s12} = \int_0^z g(\tau)\, H(\tau)\, G_s(z,\tau)\,d\tau$$

$$= \frac{1}{k^2 - 4K^2}[2h(z)\, G(z) - H(z)(1 + g(z))],$$

$$I_{s22} = \int_0^z h(\tau)\, H(\tau)\, G_s(z,\tau)\,d\tau$$

$$= \frac{1}{k^2 - 4K^2}\left[2G(z)\frac{(1 - g(z))}{k^2} - h(z)\, H(z)\right],$$

$$I_{sy11} = \int_0^z g(\tau)\, G(\tau)$$

$$= \frac{1}{k^2 - K^2}[k^2\, h(z)\, G(z) - K^2\, H(z)\, g(z)],$$

$$I_{sy12} = \int_0^z g(\tau)\, H(\tau)$$

$$= \frac{1}{k^2 - K^2}[G(z)\, g(z) + k^2\, H(z)\, h(z) - 1],$$

$$I_{sy21} = \int_0^z h(\tau)\, G(\tau)$$

$$= \frac{1}{k^2 - K^2}[1 - G(z)\, g(z) - K^2\, H(z)\, h(z)],$$

$$I_{sy22} = \int_0^z h(\tau)\, H(\tau)$$

$$= \frac{1}{k^2 - K^2}[G(z)\, h(z) - H(z)\, g(z)].$$

Acknowledgements

This work was supported in part by the Office of Naval Research. The author would like to thank the members of the Electron Physics Group, particularly Dr. J. McClelland, for stimulating discussions on this topic.

References

[1] W. Wien, Ann. Phys. **65** (1898) 444.
[2] W. H. J. Anderson, J. B. LePoole, J. Phys. **E3** (1970) 121.
[3] G. H. Curtis, J. Silcox, Rev. Sci. Instr. **42** (1971) 630.
[4] P. E. Batson, Rev. Sci. Instr. **57** (1986) 43.
[5] K. Tsuno, M. Terauchi, M. Tanaka, Optik **78** (1988) 71.
[6] H. Boersch, J. Geiger, W. Stuckel, Z. Phys. **180** (1964) 415.
[7] R. L. Seliger, J. Appl. Phys. **43** (1972) 2352.
[8] L. Holmid, Int. J. Mass Spec. Ion Phys. **17** (1975) 403.
[9] M. Saloma, H. A. Enge, Nuc. Instr. Meth. **145** (1977) 279.
[10] S. Taya, K. Tokiguchi, I. Kanomata, H. Matsuda, Nuc. Instr. Meth. **150** (1978) 165.
[11] P. S. Farago, Adv. Elec. Elec. Phys. **21** (1965) 1.
[12] S. S. Abhyankar, M. R. Bhiday, Proc. Indian Acad. Sci. **A74** (2) (1971) 53.
[13] M. J. M. Beerlage, P. S. Farago, J. Phys. **E14** (1981) 928.
[14] W. Legler, Z. Phys. **171** (1963) 424.
[15] W. H. J. Anderson, Brit. J. Appl. Phys. **18** (1967) 1573.
[16] R. DeGryse, J. P. Landuyt, G. Vervaet, J. Vennik, J. Phys. **E10** (1977) 458.
[17] J. W. Hurd, Nuc. Instr. Meth. **A258** (1978) 165.
[18] K. Kuroda, Optik **66** (1984) 355.
[19] A. Matsumoto, Mass Spectr. **33** (1985) 65.
[20] A. V. Solov'ev, A. B. Tolstoguzov, Sov. Phys. Tech. Phys. **32** (1987) 580.
[21] R. L. Seliger, J. Appl. Phys. **43** (1972) 2352.
[22] D. Ioanoviciu, Int. J. Mass. Spec. Ion. Phys. **11** (1973) 169.
[23] D. Ioanoviciu, Int. J. Mass. Spec. Ion. Phys. **15** (1973) 89.
[24] R. E. Collins, J. Vac, Sci. Technol. **10** (1973) 1106.
[25] A. Galejs, C. E. Kuyatt, J. Vac. Sci. Technol. **15** (1978) 865.
[26] T. T. Tang, Optik **74** (1986) 51.
[27] H. Rose, Optik **77** (1987) 26.
[28] X. Jiye, Adv. Elec. Elec. Phys. Supp. **17** (1986).
[29] N. Dekkers, J. Phys. **D7** (1974) 805.
[30] M. Haider, W. Bernhardt, H. Rose, Optik **63** (1982) 9.
[31] K. L. Brown, SLAC-75 (1982).
[32] R. H. Helm, SLAC-24 (1963).
[33] H. Matsuda, H. Wollnik, Nucl. Instr. Meth. **77** (1977) 40.
[34] H. Matsuda, H. Wollnik, Nucl. Instr. Meth. **77** (1977) 283.
[35] J. Kessler, Polarized Electrons, Springer-Verlag, Berlin, (1985).
[36] J. Unguris, D. T. Pierce, R. J. Celotta, Rev. Sci. Instr. **57** (1986) 1314.
[37] M. R. Scheinfein, D. T. Pierce, J. Unguris, J. J. McClelland, R. J. Celotta, M. H. Kelley, Rev. Sci. Instr. **60** (1989) 1.
[38] H. Goldstein, Classical Mechanics, Addison-Wesley, Reading, Ma (1951).
[39] N. F. Ramsey, Molecular Beams, Oxford Press, London, U.K. (1956).